Novel Contrast Agents for Magnetic Resonance Imaging. Synthesis and Characterization of the Ligand BOPTA and Its Ln(III) Complexes (Ln = Gd, La, Lu). X-ray Structure of Disodium (*TPS*-9-145337286-*C*-*S*)-[4-Carboxy-5,8,11-tris(carboxymethyl)-1-phenyl-2-oxa-5,8,11-triazatridecan-13-oato(5−)]gadolinate(2−) in a Mixture with Its Enantiomer

Fulvio Uggeri,*,† Silvio Aime,‡ Pier Lucio Anelli,† Mauro Botta,‡ Marino Brocchetta,† Christoph de Haën,† Giuseppe Ermondi,‡ Maurizio Grandi,† and Paola Paoli§

Research & Development Division, Bracco SpA, Via E. Folli 50, 20134 Milano, Italy, Dipartimento di Chimica Inorganica, Chimica Fisica e Chimica dei Materiali dell'Università di Torino, Via P. Giuria 7, 10125 Torino, Italy, and Dipartimento di Energetica dell'Università di Firenze, Via S. Marta 3, 50139 Firenze, Italy

Received June 3, 1994[⊗]

The syntheses of the ligand BOPTA, (4-carboxy-5,8,11-tris(carboxymethyl)-1-phenyl-2-oxa-5,8,11-triazatridecan-13-oic acid; benic acid) and its Gd(III), La(III), and Lu(III) complexes are reported. Protonation constants for BOPTA have been determined by potentiometry, and the microscopic protonation sequence has been investigated by ^{1}H NMR. The results obtained together with the value of the Gd-BOPTA^{2-} stability constant (log K_{ML} = 22.59) show that the complexing properties of the ligand, in comparison with DTPA, are little affected by the presence of the benzyloxymethyl residue in the structure. The solid state structure of Gd-BOPTA disodium salt $[C_{22}H_{26}N_3O_{11}(H_2O)Gd]Na_2{\cdot}^3/_2H_2O$ was determined in a single-crystal X-ray diffraction study. The structure consists of $[C_{22}H_{26}N_3O_{11}(H_2O)Gd]^{2-}$ anions, sodium cations, and water molecules; the space group is $P\bar{1}$ (Z = 2), with a = 9.083(6) Å, b = 9.469(2) Å, c = 16.698(6) Å, α = 102.22(3)°, β = 92.48(4)°, γ = 102.26(3)°, V = 1366(1) Å^3, and d = 1.84 g/mL. The gadolinium ion adopts a nine-coordinate geometry, which is best described as a distorted tricapped trigonal prism. Eight coordinating sites are occupied by the ligand (three nitrogen atoms and five carboxylate oxygens), and the ninth site is occupied by the oxygen atom of a water molecule. Relaxation studies have shown that in solution also Gd-BOPTA^{2-} has one water molecule directly coordinated to the metal ion. ^{139}La NMR studies on the La-BOPTA^{2-} complex have further supported the view that such complexes maintain in solution the same kind of coordination as found in the solid state for Gd-BOPTA disodium salt. ^{13}C NMR spectra of the diamagnetic La- and Lu-BOPTA^{2-} complexes at various temperatures are consistent with the presence of two couples of isomers interconverting through a dynamic process. Such a process has previously been reported for the parent Ln-DTPA^{2-} complexes.

Introduction

Introduction of magnetic resonance imaging (MRI) into clinical diagnosis was soon followed by the development of contrast agents capable of increasing the power of the technique.[1,2] A major class of contrast agents is paramagnetic substances which accelerate magnetic relaxation processes, primarily those of water protons. Among the paramagnetic contrast agents, Gd(III) complexes are of particular interest. The Gd(III) ion excels because of its high paramagnetism (seven unpaired electrons) and long electronic relaxation time. The gadolinium complex of diethylenetriaminepentaacetic acid, Gd-DTPA^{2-}, was the first MRI contrast agent in clinical use.[3] This complex combines favorable magnetic properties with high thermodynamic stability. The latter reduces the risk of toxicity arising from the release *in vivo* of Gd(III) ions and their subsequent interaction with biological substrates. Gd-DTPA^{2-} does not enter cells and is excreted almost exclusively by the kidney. The search for analogous complexes that *would* enter hepatocytes and which could be excreted in the bile led to a series of Gd(III) complexes being prepared that are derived from polyamino polycarboxylic chelating agents carrying various substituents.[4] Pharmacological and MRI contrast-enhancing properties indicated Gd-BOPTA^{2-} (international nonproprietary name: gadobenate) as a promising candidate,[5] the ligand BOPTA being 4-carboxy-5,8,11-tris(carboxymethyl)-1-phenyl-2-oxa-5,8,11-triazatridecan-13-oic acid. This contrast agent proved not only to be useful for the imaging of the liver and the myocardium in animals[6] but also to be more effective than Gd-DTPA^{2-} for those imaging applications which require an extracellular agent. In this paper we report (a) the synthesis, characterization, and protonation scheme of the BOPTA ligand, (b) the preparation, stability constant, and solid state X-ray structure of the Gd-BOPTA disodium salt, (c) the ability of Gd-BOPTA^{2-} to affect the longitudinal relaxation time (T_1) of bulk

† Bracco SpA.
‡ Università di Torino.
§ Università di Firenze.
⊗ Abstract published in *Advance ACS Abstracts,* December 1, 1994.

(1) (a) Lauffer, R. B. *Chem. Rev.* **1987**, *87*, 901. (b) Lauffer, R. B. *Magn. Reson. Quart.* **1990**, *6*, 65.
(2) Koenig, S. H.; Brown, R. D. *Prog. Nucl. Magn. Reson. Spectrosc.* **1990**, *22*, 487.
(3) Gries, H.; Miklautz, H. *Physiol. Chem. Phys. Med. NMR* **1984**, *16*, 105.
(4) Felder, E.; Uggeri, F.; Fumagalli, L.; Vittadini, G. Paramagnetic chelates useful for MRI imaging. U.S. Patent No. 4,916,246, April 10, 1990; IT 19236A, Jan 30, 1986.
(5) Vittadini, G.; Felder, E.; Musu, C.; Tirone, P. *Invest. Radiol.* **1990**, *25*, S59.
(6) Cavagna, F.; Daprà, M.; Maggioni, F.; de Haën, C.; Felder, E. *Magn. Reson. Med.* **1991**, *22*, 329.

0020-1669/95/1334-0633$09.00/0

solvent water, and (d) the solution structure and dynamics of the diamagnetic La- and Lu-BOPTA^{2-} complexes.

Experimental Section

Electrodialyses were carried out with a Model ED-0.4 instrument from Hydro Air Research (Zerbo di Opera, Milan, Italy) fitted with seven cation- and five anion-exchange STX membranes (total exchange surface: 0.33 m^2); voltage was set at 12 V, and the desalting procedures were prolonged until chloride ions were no longer present in the retenate (usually 4−6 h). ^{1}H and ^{13}C NMR spectra were recorded on Bruker AC 200 and JEOL EX-400 spectrometers. Fast atom bombardment (FAB) mass spectra were obtained with a VG 7070EQ mass spectrometer. Elemental analyses within commonly accepted limits (H, ±0.2%; C, N, Ln, ±0.4%) were obtained for all new compounds except for [La-BOPTA]Na_2 and [Lu-BOPTA]Na_2.

Organic and inorganic reagents, including D_2O, were purchased from E. Merck, Darmstadt, Germany, and used without further purification. Gd_2O_3, $LuCl_3{\cdot}6H_2O$, and $LaCl_3$ were obtained from Aldrich (Milan, Italy). DCl and NaOD were purchased from Sigma Chimica (Milan, Italy). 2-Chloro-3-(phenylmethoxy)propanoic acid was prepared according to the procedure of Grassman *et al.* for the bromo analogue.[7]

***N*-[2-[(2-Aminoethyl)amino]ethyl]-*O*-(phenylmethyl)-DL-serine Tris(hydrochloride) (1·3HCl).** 2-Chloro-3-(phenylmethoxy)propanoic acid (42.9 g, 200 mmol) was added over 10 min to a solution of diethylenetriamine (269 g, 2.58 mol) in H_2O (400 mL). The mixture was stirred at 50 °C for 40 h and then cooled to room temperature before being loaded onto a column of Amberlite IRA 400 (1.8 L; OH^- form). The column was eluted first with H_2O to remove excess diethylenetriamine and then with 1 N HCl. The acidic solution (4 L) was collected and evaporated to dryness. The crude oil was crystallized from EtOH to give **1**·3HCl (45.5 g; 58%) as a white solid: mp 163−165 °C; ^{13}C NMR (DMSO-d_6) δ 35.0, 41.6, 42.3, 43.8, 59.1, 66.4, 72.5, 127.7, 128.3, 137.3, 168.2. Anal. Calcd for $C_{14}H_{26}Cl_3N_3O_3$: C, 43.03; H, 6.71; N, 10.75; Found: C, 43.05; H, 6.63; N, 10.82.

4-Carboxy-5,8,11-tris(carboxymethyl)-1-phenyl-2-oxa-5,8,11-triazatridecan-13-oic Acid (BOPTA). NaOH (5 N; 165 mL) was added to a stirred solution of bromoacetic acid (115 g, 0.825 mol) in H_2O (250 mL) maintained at 0−5 °C. After the mixture was heated to 50 °C, a solution of **1**·3HCl (49.6 g, 0.127 mol) in 2 N NaOH (255 mL) was added over 30 min, and the resulting solution was stirred at 50 °C for 8 h. During this time, a pH of 10 was maintained by continuous addition of 2 N NaOH. The reaction solution was stirred at room temperature for 15 h and loaded onto a column of Amberlite IR 120 (2.1 L; H^+ form). This was eluted first with H_2O and then with 2 N NH_4OH. The alkaline solution containing the product was evaporated to dryness; the oily residue was dissolved in H_2O (450 mL), and then the pH of the solution was adjusted to 1.7 by addition of concentrated HCl. After 6 d, the solid was filtered off, washed with H_2O (2 × 40 mL), and dried *in vacuo* over P_2O_5. The white solid thus obtained was **BOPTA** (13.8 g, 21%): mp 118 °C; ^{1}H NMR (D_2O, pD_{app} 3; *vide infra*) δ 3.3 (bt, 2H), 3.35 (bt, 2H), 3.4 (bt, 4H), 3.9−4.0 (m, 10H), 4.2 (t, 1H), 4.5−4.6 (dd, 2H), 7.3−7.4 (m, 5H); ^{13}C NMR (DMSO-d_6) δ 49.3, 50.1, 51.7, 52.4, 53.4, 54.5, 54.9, 64.1, 69.6, 72.4, 127.5, 128.2, 138.0, 168.5, 172.5, 172.6, 174.4; MS (FAB+) *m/z* 514 [M + H]$^+$. Anal. Calcd for $C_{22}H_{31}N_3O_{11}$: C, 51.46; H, 6.08; N, 8.18; Found: C, 51.28; H, 6.12; N, 8.13.

Gd-BOPTA Disodium Salt. BOPTA (25.7 g, 50.0 mmol) was suspended in H_2O (150 mL) and dissolved by addition of 1 N NaOH (100 mL, 0.1 mol). After addition of Gd_2O_3 (9.06 g, 25.0 mmol), the suspension was stirred at 80 °C for 1.5 h. The formation of the complex was monitored by HPLC [E. Merck LiChrospher 100 RP-8, 5 μm, 250 × 4 mm column, thermostated at 40 °C; eluant aqueous solution of MeCN (27% v/v), containing 1 g/L of *n*-octylamine and buffered at pH 6.0 with H_3PO_4; flow rate 1 mL min^{-1}] and by titration of the free ligand. The turbid solution was filtered through a Millipore Durapore membrane (0.45 μm) filter and evaporated to dryness. The residue was then dried *in vacuo* (P_2O_5; 2 kPa; 50 °C) to give **Gd-BOPTA disodium salt** in almost quantitative yield: mp >250 °C. Anal. Calcd for $C_{22}H_{26}GdN_3Na_2O_{11}$: C, 37.13; H, 3.68; N, 5.90; Gd, 22.10. Found (after drying the product at 230 °C): C, 37.06; H, 3.74; N, 5.88; Gd, 22.48.

Gd-BOPTA bis(*N*-methylglucammonium) salt was prepared according to the procedure described for the disodium salt but with *N*-methylglucamine instead of NaOH; mp 124 °C. Anal. Calcd for $C_{36}H_{62}GdN_5O_{21}$: C, 40.86; H, 5.92; N, 6.62; Gd, 14.86. Found: C, 40.77; H, 6.08; N, 6.63; Gd, 14.84.

Lu-BOPTA Disodium Salt. BOPTA (15.4 g, 30.0 mmol) was dissolved in H_2O (100 mL) by the addition of 2 N NaOH (2.3 mL, 46 mmol), and a solution of $LuCl_3{\cdot}6H_2O$ (11.7 g, 30.0 mmol) in H_2O (20 mL) was added. NaOH (2 N; 5.20 mL, 104 mmol) was added slowly and the reaction mixture (pH 6.5) stirred at room temperature for 3 h. The cloudy solution was filtered through a Millipore Durapore membrane (0.45 μm) filter and desalted by electrodialysis. The pH was adjusted to 6.5 with 1 N NaOH, and then the solution was evaporated *in vacuo*. The residue was dried (P_2O_5; 50 °C; 2 kPa), and **Lu-BOPTA disodium salt** was obtained as a white solid (16.5 g; 75%): mp >250 °C. Anal. Calcd for $C_{22}H_{26}LuN_3Na_2O_{11}$: C, 36.23; H, 3.60; N, 5.76; Lu, 23.99; Na, 6.30. Found: C, 36.72; H, 3.67; N, 5.79; Lu, 23.88; Na 6.34. Despite the high carbon value, the material was considered sufficiently pure for the limited purpose of this study.

La-BOPTA disodium salt was prepared according to the procedure described for the lutetium complex: yield 93%; mp >250 °C; Anal. Calcd for $C_{22}H_{26}LaN_3Na_2O_{11}$: C, 38.11; H, 3.78; N, 6.06; La, 20.03; Na, 6.63. Found: C, 37.86; H, 3.83; N, 5.93; La, 19.40; Na, 6.39. Despite the low lanthanum value, the material was considered sufficiently pure for the limited purpose of this study.

Potentiometry and Stability Constant Determination. Protonation constants for BOPTA defined as

$$K_{H_nL} = [H_nL]/[H_{n-1}L][H^+] \quad n = 1-5$$

were determined by potentiometric titrations at 20.0 ± 0.1 °C and μ = 0.1 M (KCl). The ligand solution (20 mL, 0.001 M) was titrated in a thermostated cell under a stream of nitrogen with a 0.1 *M* standard solution of KOH added by means of a 1 mL piston buret. Potentiometric measurements were carried out with a Metrohm E 636 potentiometer equipped with a Metrohm glass electrode and a thermostated calomel (KCl saturated) reference electrode. Prior to each potentiometric equilibrium study, the glass electrode was calibrated as a hydrogen concentration probe by titration of a known amount of HCl with 0.1 M KOH and determining the equivalent point by the method of Gran.[8] This allows us to evaluate the standard potential $E°$ and the ionic product of water K_w. The stability constant of Gd-BOPTA^{2-} defined as

$$K_{Gd-BOPTA^{2-}} = [Gd\text{-}BOPTA^{2-}]/[Gd^{3+}][BOPTA^{5-}]$$

was determined at 20 °C by potentiometry in the presence of auxiliary chelants of known stability constants such as EDTA and DTPA. These experiments were performed at [BOPTA] = 0.001 M with ratios [BOPTA]:[$GdCl_3$]:[auxiliary ligand] from 1:1:1 to 1:1:4. The ligand protonation constants and complex stability constants for Gd-BOPTA^{2-} were obtained from the experimental potentiometric data using the software SUPERQUAD.[9] Calculations were based on the published values for the stability constants of Gd-EDTA$^-$ and Gd-DTPA^{2-}, i.e. log K = 17.37 (μ = 0.1 M; KNO_3) and log K = 23.01 (μ = 0.1 M; KCl), respectively.[10,11] Protonation constants were obtained by treating the five best titration curves as separate entities. Stability constants for Gd-BOPTA^{2-} were calculated by treating as separate entities three measurements for each [BOPTA]:[$GdCl_3$]:auxiliary ligand] ratio which had been used.

Collection and Reduction of X-ray Diffraction Intensity Data. Prismatic colorless crystals of the $[C_{22}H_{26}N_3O_{11}(H_2O)Gd]Na_2{\cdot}^3/_2H_2O$

(7) Grassman, W.; Wünsch, E.; Deufel, P.; Zwick, A. *Chem. Ber.* **1958**, *91*, 538.

(8) Gran, G. *Analyst* **1952**, *77*, 661.

(9) Gans, P.; Sabatini, A.; Vacca, A. *J. Chem. Soc, Dalton Trans* **1985**, 1195.

(10) Schwarzenbach, G.; Gut, R.; Anderegg, G. *Helv. Chim. Acta* **1954**, *37*, 937.

(11) Harder, R; Chaberek, S. *J. Inorg. Nucl. Chem.* **1959**, *11*, 197.

compound which proved suitable for X-ray diffraction analysis were obtained by slow crystallization from a 1:1 (v/v) DMSO−H_2O solution. Concentrations between 100 and 200 mg/mL were used, and crystallization took place at 50 °C. A crystal of approximately 0.2 × 0.4 × 0.6 mm^3 was attached with epoxy glue to a glass fiber and mounted on an Enraf-Nonius CAD4 X-ray diffractometer using the equatorial geometry. Cell constants were determined by least-squares fitting of 25 accurately centered reflections. During data collection, the intensities of three standard reflections were checked periodically for stability, and no loss of intensity was observed. A total of 5019 reflections were collected in the range $5 < 2\theta < 50°$, corresponding to the Miller indices $-10 \le h \le 10$, $-11 \le k \le 11$, and $0 \le l \le 19$, by using Mo K-$L_{2,3}$ graphite-monochromated radiation. The data set was corrected for Lorentz and polarization effects, and once the structure was solved, an absorption correction was applied by using the method of Walker and Stuart.[12]

Solution and Refinement of the Structure. A total of 4184 independent reflections with $I > 3\sigma(I)$ was used for the solution and refinement of the structure. The structure was solved by the heavy-atom method: the Patterson map showed the gadolinium ion. Subsequent F_o and ΔF Fourier syntheses revealed the positions of all non-hydrogen atoms; the hydrogen atoms of the ligand were introduced into calculated (unrefined) positions with an overall temperature factor, U, of 0.06 $Å^2$. All other atoms were refined using anisotropic temperature factors. The oxygen atom O14 of a molecule of water of crystallization was refined with an occupancy factor of 0.5. Refinement was performed by the full-matrix least-squares method to $R = 0.037$ and $R_w = 0.033$. The minimized function was $\sum w(|F_o| - |F_c|)^2$, with $w = a/\sigma^2(F)$, where a is an iteratively adjusted parameter. All calculations were performed on a IBM PS/2 80 computer with the SHELX-76 set of programs.[13] These use the analytical approximation described in ref 14 for the atomic scattering factors and anomalous dispersion corrections for each atom. The molecular plots were produced by the program ORTEP.[15] Bond distances and angles were calculated with the program PARST.[16]

Relaxivity Measurements. Water proton relaxation measurements (39 °C, 20 MHz) were carried out with a Bruker Minispec PC120 instrument on five solutions (0.1−5.0 mM) of Gd-BOPTA and Gd-DTPA bis(*N*-methylglucammonium) salts. Spin−lattice relaxation times, T_1, were measured by the inversion recovery method. After setting the instrument to measure the decay of the signal down to 33% of the initial value, spin−spin relaxation times, T_2, were determined by the Carr−Purcell−Meiboom−Gill (CPMG) pulse sequence.[17] Relaxivities r_i were calculated from the slope of the regression line of $1/T_i$ vs concentration (least-squares method).

The $1/T_1$ nuclear magnetic resonance dispersion (NMRD) profiles[18] of water protons were measured using 1.5 mM solutions of the disodium salts of the Gd complexes over a continuum of magnetic flux densities from 2.5×10^{-4} to 1.4 T (corresponding to 0.01−50 MHz proton Larmor frequencies). A Koenig-Brown relaxometer was used which is installed at the Department of Chemistry at the University of Florence (Italy). The reproducibilities of the measured T_1 values were ±1%.

NMR Spectral Measurements. Solutions of the ligand (0.1 M) for the NMR acid/base titrations were made up in D_2O (99.8%), and the apparent pD was adjusted with DCl or NaOD. Apparent pD_{app} was measured with a glass combination electrode standardized with H_2O on the basis of pH buffers. Since the corrections needed to convert apparent into real pD are not yet known for the full pH/pD scale, observed values for pD_{app} were taken without correction. Proton spectra were recorded at 25 ± 0.5 °C and 400 MHz on a JEOL EX-400 spectrometer, and the chemical shifts were referenced to Me_4Si. Solutions of the La-BOPTA^{2-} and Lu-BOPTA^{2-} complexes (0.15 M) were prepared in D_2O, and the apparent pD_{app} was adjusted to 7.4 with NaOD. ^1H, ^{13}C, and ^{139}La NMR spectra were obtained on a JEOL EX-400 spectrometer. The variable-temperature accessory was calibrated with methanol,[17] and before measurements were taken, the NMR samples were allowed to equilibrate in the probe for about 15 min. *tert*-Butyl alcohol (1%) was used as an internal chemical shift standard for proton and carbon spectra, while the ^{139}La resonances were referenced to a solution of $LaCl_3$ confined to a closed capillary inside the NMR tube.

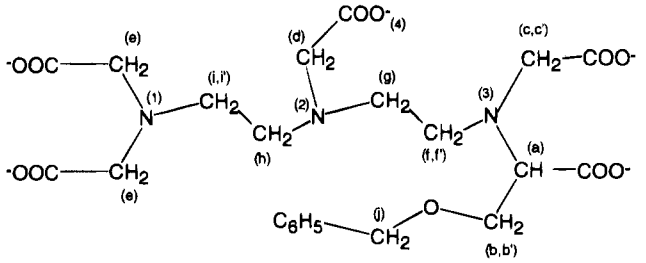

Figure 1. BOPTA^{5-}: labeled structure.

Table 1. Potentiometric Protonation Constants for BOPTA, DTPA, and EDTA[a,b]

	BOPTA	DTPA[c]	EDTA[c]
$\log K_{HL}$	10.71 (0.03)	10.55 (0.03)	10.24 (0.02)
$\log K_{H_2L}$	8.27 (0.03)	8.59 (0.01)	6.16 (0.02
$\log K_{H_3L}$	4.35 (0.02)	4.30 (0.04)	2.66 (0.02)
$\log K_{H_4L}$	2.83 (0.02)	2.66 (0.1)	2.0 (0.1)
$\log K_{H_5L}$	2.07 (0.05)	1.82 (0.04)	

[a] At 20 °C, μ = 0.1 M (KCl). [b] Estimated standard deviations in parentheses. [c] From ref 19.

Results and Discussion

Synthesis. The ligand BOPTA was prepared in two steps. First, diethylenetriamine was selectively monoalkylated on a primary amino group with 2-chloro-3-(phenylmethoxy)propanoic acid in water and the intermediate isolated as the tris(hydrochloride). In the second step, the intermediate was fully carboxymethylated with bromoacetic acid in water at pH 10 to give BOPTA. The gadolinium complex was prepared with Gd_2O_3. The lanthanum and lutetium complexes were prepared from the corresponding chlorides and were purified by electrodialysis.

BOPTA Protonation Constants. The values for the macroscopic protonation constants of BOPTA, which were calculated from the potentiometric titration curves, are reported in Table 1 together with the values for structurally related linear polyamino polycarboxylic ligands. The very similar values found for BOPTA and DTPA indicate that the substitution of a hydrogen atom on a terminal acetic group with a benzyloxymethyl residue does not alter substantially the basicity of the protonation sites. The ionic species distribution diagram as a function of pH, which was calculated with the help of the potentiometric protonation constants, is reported in Figure 2a.

In NMR, protonation of a basic site on a polyamino polycarboxylic ligand results in a deshielding of the adjacent nonlabile protons. Therefore, the microscopic protonation sequence may be analyzed by measuring the variation of chemical shift values of nonlabile protons of the ligand as a function of the solution acidity.[20,21]

(12) Walker, N.; Stuart, D. D. *Acta Crystallogr., Sect. A* **1983**, *39*, 158.
(13) Sheldrick, G. M. *SHELX-76, Program for Crystal Structure Determination;* University of Cambridge: Cambridge, England, 1976.
(14) *International Tables for X-ray Crystallography*; Kynoch: Birmingham, England, 1974; Vol. IV.
(15) Johnson C. K. ORTEP. Report ORNL-3794; Oak Ridge National Laboratory: Oak Ridge, TN, 1971.
(16) Nardelli M. PARST. *Comput. Chem.* **1983**, *7*, 95.
(17) Martin, M. L.; Delpeuch, J. J.; Martin, G. J. *Practical NMR Spectroscopy*; Heyden: Chichester, England, 1980.
(18) Koenig, S. H.; Brown, R. D. In *NMR Spectroscopy of Cells and Organisms*; Gupta, R. K., Ed.; CRC Press: Boca Raton, FL, 1987; Vol. II, p 75.
(19) Martell, A. E.; Smith, R. M. *Critical Stability Constants*; Plenum Press: New York and London, 1974; Vol. 1.
(20) Sudmeier, J. L.; Reilley, C. N. *Anal. Chem.* **1964**, *36*, 1698.
(21) Ascenso, J. R.; Delgado, R.; da Silva, J. J. R. *J. Chem. Soc., Perkin Trans. 2* **1985**, 781.

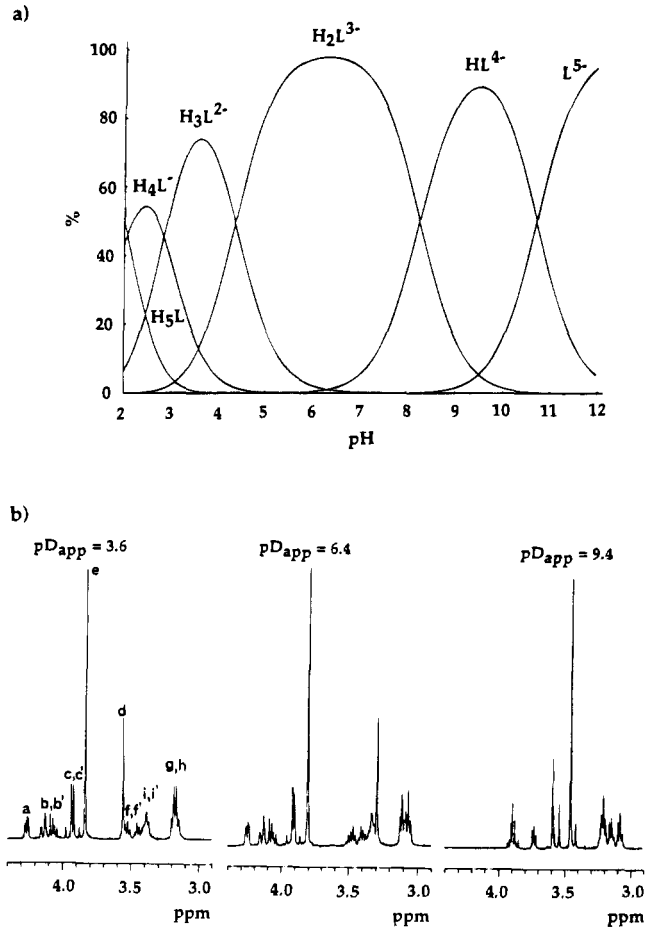

Figure 2. (a) Distribution, determined potentiometrically, of the protonated species of BOPTA as a function of pH. (b) ^{1}H NMR spectra of BOPTA at selected pD_{app} values.

Representative proton spectra at selected pD_{app} values (see Experimental Section) are reported in Figure 2b (labeling of nonlabile protons is in accord with Figure 1). The signals were assigned on the basis of assignments for other polyamino polycarboxylic ligands,[20] the integration of the resonances, and conventional homo- and heteronuclear COSY 2D experiments. Experimental data for the chemical shifts of CH_2COO^- (e, d, c,c') and $CHRCOO^-$ (a) proton resonances vs pD_{app} are reported in Figure 3. From analysis of the chemical shift variation, especially of the d protons, three inflection points can be seen, indicating that three protonation steps must occur on the ligand over the studied pD_{app} range.

The observed chemical shift for proton i is given by

$$ {}^i\delta_{obs} = \sum_n {}^i\delta_n X_{H_nL} \qquad (1) $$

where ${}^i\delta_n$ are the proton chemical shifts related to the H_nL protonated species and X_{H_nL} is the mole fraction of each species.[22] The equations describing the first three steps (n = 3) of protonation of the ligand were fit simultaneously to all the data. This was achieved using a function (see eq 2) obtained

$$ f({}^i\delta_{obs}) = \sum_i {}^i\delta_{obs}\, {}^i m \qquad (2) $$

from the linear combination of all equations of type (1), each

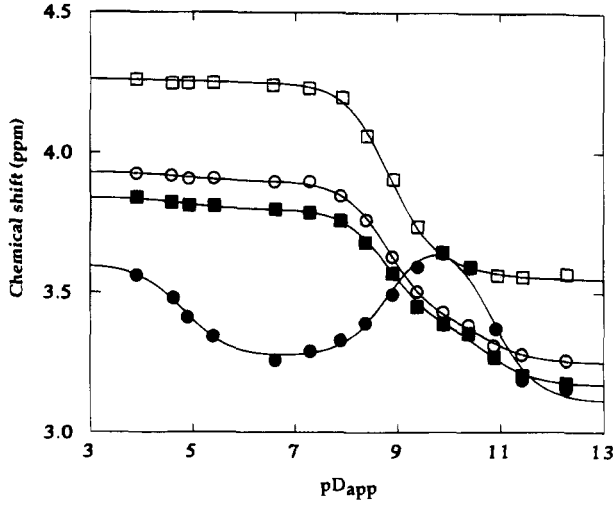

Figure 3. ^{1}H NMR titration curves for BOPTA. Selected resonances: a (□); c,c' (○); d (●); e (■). Solid lines were calculated from the equations describing the first three protonation steps of $BOPTA^{5-}$ using the best fit parameters shown in Table 2.

weighted by a "dummy" variable, ${}^i m$,[23] where ${}^i m$ can be either 0 or 1. In this way a unique residual sum of squares and a unique set of parameters according to the criterion of least squares can be calculated. Results in terms of ${}^i\delta$ for the H_nL species are reported in Table 2, and the calculated curves are drawn in Figure 3. These protonation constants obtained in D_2O, i.e. log K_{DL} = 10.80 (0.08), log K_{D_2L} = 8.85 (0.04), and log K_{D_3L} = 4.82 (0.09), are necessarily higher than those obtained in water by potentiometry because the deuteron interacts more strongly with oxygen and nitrogen atoms than the proton. Especially if one considers that in the two experiments different ligand concentrations and ionic strengths have been used and that only an apparent pD was estimated (see Experimental Section), the similarities between pK_H and pK_D values are satisfactory. Thus the data on the protonation sequence in D_2O can be extrapolated to the situation in water. It is worth noting that, unlike what has previously been reported by other authors, ${}^i\delta$ for the H_nL species are calculated in our procedure without using protonation constants determined by potentiometry.

The procedure of Sudmeier and Reilley,[20] which is based on empirical shielding constants for protons as a function of the distance from a charged residue, was used to gain further insights into the protonation mechanism. The BOPTA structure contains seven unequivalent basic sites, and there are three usable CH_2 resonances, i.e. c,c', d, e. The CH proton resonance cannot be exploited because shielding constants for such protons have never been determined for model compounds. Therefore, to minimize the number of unknowns, calculations have been performed under the hypothesis that only nitrogen atoms are involved in the first and second protonation steps. However, in this way, variables f_j (the average time fraction during which the jth basic site is protonated; see Figure 1 for labeling) become overdetermined. The most appropriate set is chosen by minimizing the sums of the squares of the differences between the previously determined ($\Delta^i\delta$) and the calculated ($\Delta^i\delta_{SR}$) values, considering that ${}^i\delta_{SR}$ are the ${}^i\delta$ values according to the Sudmeier and Reilley procedure.[20]

Because the third protonation step is likely to partially involve the carboxylate functions, the number of f_j variables becomes

(22) Geraldes, C. F. G. C.; Sherry, A. D.; Cacheris, W. P. *Inorg. Chem.* **1989**, *28*, 3336.

(23) Draper, N. R.; Smith, H. *Applied Regression Analysis*, 2nd ed.; John Wiley & Sons: New York, 1981.

(24) *SAS/STAT User's Guide*, Release 6.03; SAS Institute Inc.: Cary, NC, 1988.

Table 2. Best Fit Values of ^{1}H Chemical Shifts ($^i\delta$)[a,b] Deduced from ^{1}H NMR Titration Data for BOPTA in D_2O (Figure 3) Together with $^i\delta_{SR}$ and f_j[c] As Determined by the Sudmeier and Reilley Procedure[d]

								f_j, %			
n	$^e\delta$	$^e\delta_{SR}$	$^d\delta$	$^d\delta_{SR}$	$^{c,c'}\delta$	$^{c,c'}\delta_{SR}$	$^a\delta$	f_1	f_2	f_3	f_4
0	3.17	3.30	3.11	3.30	3.25	3.30	3.55				
1	3.38	3.43	3.73	3.85	3.40	3.37	3.59	18.7	74.7	11.4	
2	3.80	3.92	3.27	3.47	3.90	3.94	4.25	85.6	23.6	89.3	
3	3.84	3.96	3.60	3.79	3.93	3.98	4.26	88.6	44.9	90.6	75.8

[a] Calculations were performed using the statistical software package SAS.[24] The variance explained [defined as 1 − (residual sum of squares/total sum of squares)] was 0.9983. [b] The alphabetical superscripts of the chemical shifts refer to the proton identification (see Figure 1). [c] The numerical subscripts refer to the protonation sites (see Figure 1). [d] $^a\delta_{SR}$ were not determined as *CH* protons cannot be used in the Sudmeier and Reilley procedure.

Table 3. Gd-BOPTA^{2-} Stability Constants Determined by Competition Experiments with Other Ligands

[BOPTA]:[Gd^{3+}]:[H_jX]	H_jX	log $K_{Gd-BOPTA^{2-}}$[a]
1:1:1	EDTA	22.53 (0.01)
1:1:2	EDTA	22.58 (0.02)
1:1:4	EDTA	22.61 (0.04)
1:1:1	DTPA	22.64 (0.04)
		22.59 (0.04)[b]

[a] Estimated standard deviations in parentheses. [b] Average value.

too high. However, from Figure 3 it can be seen that, at pH's lower than 6, the most affected resonance is that belonging to the d protons. This can be interpreted as meaning that the carboxylate on the central nitrogen atom is partially involved in the third protonation step. Under this hypothesis, with the number of unknowns equal to the number of equations, f_j values can easily be determined. Results are reported in Table 3 and quantitatively reflect that which can be seen, qualitatively, in Figure 3. From these data the following can be inferred: (i) The first protonation of BOPTA (L → DL) occurs at the central nitrogen atom. (ii) Double protonation (L → D_2L) leads to a species which carries the positive charges on the two terminal nitrogen atoms of the diethylenetriamine moiety of the molecule. The shift of the first proton from the central to a terminal nitrogen atom is driven by electrostatic repulsion of the incoming second proton. (iii) Triple protonation (L → D_3L) may include not only a molecular species with three protonated nitrogen atoms but also another species with the two protonated terminal nitrogen atoms and the third proton on the carboxyl group linked to the central nitrogen atom. This protonation sequence reflects that which was previously found for DTPA.[20] This means that the incorporation of the benzyloxymethyl residue into a terminal acetic group in the basic structure of DTPA does not affect the protonation sequence of the ligand.

Gd-BOPTA^{2-} Stability Constant. Potentiometric data on competition complexation experiments with auxiliary ligands, such as EDTA and DTPA, were analyzed, and the results are reported in Table 3. A conditional stability constant of log K^*_{ML} = 18.4 for Gd-BOPTA^{2-}, under physiologically relevant conditions, i.e. at pH 7.4, 20 °C, and μ = 0.1 M (KCl), was calculated[25] on the basis of the protonation constants of the ligand (see above).

Crystal Structure. Although crystallization of the bis(*N*-methylglucammonium) salt of Gd-BOPTA^{2-}, the product in clinical development as an MRI contrast agent, so far has been unsuccessful, crystals of the sodium salt $[C_{22}H_{26}N_3O_{11}(H_2O)Gd]Na_2{\cdot}^3/_2H_2O$, which are suitable for X-ray diffraction analysis, have been obtained. Table 4 summarizes the crystallographic and refinement data. Table 5 lists the final atomic coordinates and the equivalent temperature factors for the non-hydrogen atoms. Table 6 reports the bond distances and angles involving the gadolinium ion.

Table 4. Crystallographic Data for $[C_{22}H_{26}N_3O_{11}(H_2O)Gd]Na_2{\cdot}^3/_2H_2O$

chem formula	$C_{22}H_{31}N_3GdNa_2O_{13.5}$
fw	756.73
space group	$P\bar{1}$
a, Å	9.083(6)[a]
b, Å	9.469(2)
c, Å	16.698(6)
α, deg	102.22(3)
β, deg	92.48(4)
γ, deg	102.26(3)
v, Å^3	1366(1)
Z	2
F(000)	756
μ, cm^{-1}	25.4
abs cor	1.092−0.897
D, g cm^{-3}	1.84
radiation	graphite monochromated Mo K−$L_{2,3}$ (λ = 0.7107 Å)
temp, °C	25
$R = \sum\|\|F_o\| - \|F_c\|\|/\sum\|F_o\|$	0.037
$R_w = [\sum w(\|F_o\| - \|F_c\|)^2/\sum w(F_o)^2]^{1/2}$	0.033

[a] In parentheses are given the standard errors in terms of the last reported figure.

The crystals contain $[C_{22}H_{26}N_3O_{11}(H_2O)Gd]^{2-}$ anions, sodium cations, and water of crystallization molecules. Since the space group $P\bar{1}$ is centrosymmetric and there are two molecules per unit cell, two enantiomeric forms (see later) of the Gd-BOPTA complex must be present in the crystal. According to the guidelines of *Chemical Abstracts*,[26] the stereoisomer reported in Figure 4 may be stereochemically described by adding the prefix (*TPS*-9-145337286-*C*-*S*)- to the systematic name. Its symmetrical counterpart in the unit cell is identified by the prefix (*TPS*-9-145337286-*A*-*R*)-.

In Gd-BOPTA^{2-} the gadolinium ion is surrounded by the ligand and adopts a nine-coordinate geometry (Figure 4). The coordination sphere, which comprises the three amine nitrogens (N1, N2, N3), five carboxylic oxygens of the acetate residues (O2, O5, O6, O9, O10), and a water molecule (O12), results in a distorted tricapped trigonal prism around the metal ion. Atoms O2, O10, O5, and O6, O9, N2 form the two triangular faces, and the cap positions are occupied by the outer amine nitrogens N1 and N3 and the coordinated water oxygen (O12) (Figure 5). The dihedral angles formed by the mean least-squares planes describing the faces of the polyhedron (Table 7) agree well with those calculated for an ideal D_{3h} geometry.[27] This coordination geometry cold also be described by a square capped antiprism where the coordinated water molecule is at the cap position.

(25) de Haën, C.; Gozzini, L. *J. Magn. Reson. Imag.* **1993**, *3*, 179.

(26) *Chemical Abstracts: Index Guide*, 11th Collective Index; American Chemical Society: Columbus, OH, 1987; Appendix IV.

(27) Guggenberger, L. J.; Muetterties, E. L. *J. Am. Chem. Soc.* **1976**, *98*, 7221.

Table 5. Fractional Atomic Coordinates and Equivalent Temperature Factors for $[C_{22}H_{26}N_3O_{11}(H_2O)Gd]Na_2{}^{*3}/_2H_2O$[a]

atom	$10^4x/a$	$10^4y/b$	$10^4z/c$	10^3U, Å^2
Gd	2534(1)	2015(1)	3584(1)	13(1)
Na1	6282(3)	4245(3)	4374(2)	33(2)
Na2	7806(4)	1335(3)	5113(2)	44(2)
N1	3487(5)	−65(5)	2385(3)	17(3)
N2	354(5)	618(5)	2480(3)	16(3)
N3	1186(6)	3892(6)	3079(3)	18(3)
O1	4204(5)	−2821(5)	1736(3)	33(3)
O2	4929(5)	1564(5)	3833(3)	25(3)
O3	6447(5)	18(5)	3874(3)	32(3)
O4	5996(6)	3060(6)	1911(4)	59(4)
O5	3872(5)	2913(5)	2546(3)	35(3)
O6	1440(5)	−384(5)	3766(3)	24(3)
O7	−567(6)	−2220(6)	3661(3)	50(3)
O8	−1559(5)	3418(5)	4578(3)	30(3)
O9	281(5)	2271(5)	4230(3)	25(3)
O10	3641(4)	4596(5)	4197(3)	21(3)
O11	3949(5)	6995(5)	4189(3)	26(3)
O12	2977(5)	2147(6)	5067(3)	37(3)
O13	6827(5)	5455(6)	3291(3)	43(3)
O14	7250(11)	1875(12)	448(6)	48(7)
C1	6200(9)	−3568(8)	899(5)	33(5)
C2	6298(10)	−2510(10)	445(5)	56(6)
C3	7558(12)	−2142(12)	18(6)	73(7)
C4	8696(12)	−2833(11)	55(7)	66(7)
C5	8664(11)	−3852(11)	520(6)	66(7)
C6	7402(10)	−4222(10)	952(6)	52(6)
C7	4794(8)	−4043(8)	1315(5)	35(5)
C8	5160(8)	−1896(7)	2434(4)	25(4)
C9	4294(7)	−826(7)	2892(4)	18(3)
C10	5333(7)	349(7)	3582(4)	22(4)
C11	4511(8)	681(7)	1864(4)	25(4)
C12	4831(8)	2367(8)	2136(4)	28(4)
C13	2095(7)	−1024(7)	1907(4)	20(4)
C14	1008(7)	−83(7)	1739(4)	22(4)
C15	−636(7)	−540(7)	2808(4)	25(4)
C16	132(8)	−1122(8)	3447(4)	25(4)
C17	−518(7)	1636(7)	2237(4)	23(4)
C18	478(7)	3158(7)	2249(4)	24(4)
C19	16(7)	4283(7)	3638(4)	24(4)
C20	−457(7)	3228(7)	4189(4)	18(4)
C21	2336(7)	5238(7)	3088(4)	20(4)
C22	3381(7)	5674(7)	3882(4)	20(4)

[a] Estimated standard deviations in parentheses.

This model, however, does not fit as well as the tricapped trigonal prism to the geometrical arrangement of the donor atoms around the metal ion, especially because of the rather large shift from their least-squares plane of N1, N2, N3, and O5 atoms (maximal deviation 0.189(5) Å for the O5 atom).

According to Guggenberger and Muetterties,[27] the D_{3h} tricapped trigonal prism is the preferred polytopal form of ML_9 coordination complexes. Several solid state structures of Gd(III) complexes with polyamino polycarboxylic ligands[3,28-30] containing eight donor sites have been reported. It has turned out that, for Gd(III) complexes with acyclic ligands, the preferred geometry is the D_{3h} polyhedron[30] whereas, for Gd(III) complexes with cyclic ligands derived from the basic structure of 1,4,7,-10-tetraazacyclododecane-1,4,7,10-tetraacetic acid (DOTA), the preferred geometry is the C_{4v} capped square antiprism.[28,29] The latter geometry is favored probably because of the preorganization and the constraint of the four nitrogen atoms in the 1,4,7,-10-tetraazacyclododecane ring.

(28) Dubost, J.-P.; Leger, J.-M.; Langlois, M.-H.; Meyer, D.; Schaefer, M. *C. R. Acad. Sci. Paris* **1991**, [2] *312*, 349.
(29) Aime, S.; Anelli, P. L.; Botta, M.; Fedeli, F.; Grandi, M.; Paoli, P.; Uggeri, F. *Inorg. Chem.* **1992**, *31*, 2422.
(30) Konings, M. S.; Dow, W. C.; Love, D. B.; Raymond, K. N.; Quay, S. C.; Rocklage, S. M. *Inorg. Chem.* **1990**, *29*, 1488.

Table 6. Primary Coordination Sphere Bond Distances and Angles for the $[C_{22}H_{26}N_3O_{11}(H_2O)Gd]^{2-}$ Complex[a]

Bond Distances (Å)			
Gd−N1	2.800(5)	Gd−O6	2.367(5)
Gd−N2	2.571(5)	Gd−O9	2.388(5)
Gd−N3	2.615(6)	Gd−O10	2.416(4)
Gd−O2	2.340(5)	Gd−O12	2.463(5)
Gd−O5	2.361(5)		
Bond Angles (deg)			
O10−Gd−O12	74.7(2)	N3−Gd−O6	128.3(2)
O9−Gd−O12	70.6(2)	N3−Gd−O5	71.1(2)
O9−Gd−O10	89.2(2)	N3−Gd−O2	142.2(2)
O6−Gd−O12	74.3(2)	N2−Gd−O12	133.7(2)
O6−Gd−O10	148.4(2)	N2−Gd−O10	135.0(2)
O6−Gd−O9	75.1(2)	N2−Gd−O9	74.9(2)
O5−Gd−O12	137.7(2)	N2−Gd−O6	67.6(2)
O5−Gd−O10	75.3(2)	N2−Gd−O5	88.5(2)
O5−Gd−O9	137.6(2)	N2−Gd−O2	130.6(2)
O5−Gd−O6	134.0(2)	N2−Gd−N3	69.8(2)
O2−Gd−O12	71.8(2)	N1−Gd−O12	122.3(2)
O2−Gd−O10	87.0(2)	N1−Gd−O10	131.8(2)
O2−Gd−O9	141.8(2)	N1−Gd−O9	138.1(2)
O2−Gd−O6	88.9(2)	N1−Gd−O6	71.8(2)
O2−Gd−O5	77.6(2)	N1−Gd−O5	62.9(2)
N3−Gd−O12	120.2(2)	N1−Gd−O2	62.3(2)
N3−Gd−O10	65.2(2)	N1−Gd−N3	117.5(2)
N3−Gd−O9	66.6(2)	N1−Gd−N2	68.1(2)

[a] Estimated standard deviations of last reported digit in parentheses.

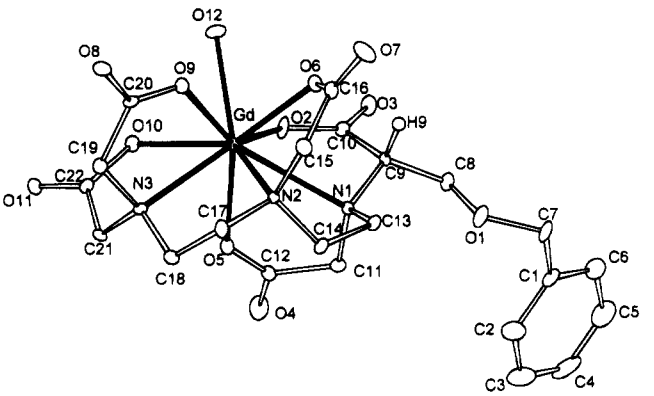

Figure 4. Solid state structure of Gd-BOPTA disodium salt. For the sake of clarity, only the hydrogen atom on the asymmetric carbon (C9) is shown.

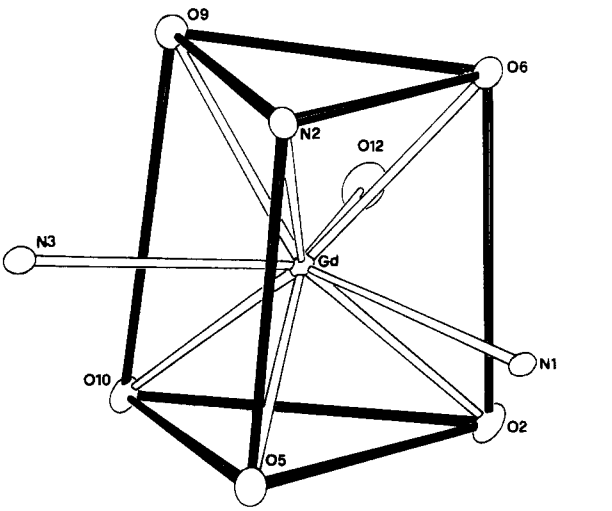

Figure 5. Coordination polyhedron about the Gd(III) ion.

The metal ion is located close to the center of the trigonal prism, slightly shifted toward the face capped by the coordinated water molecule (about 0.2 Å closer) and shifted down toward

Table 7. Dihedral Angles for $[C_{22}H_{26}N_3O_{11}(H_2O)Gd]^{2-}$

face 1	face 2	angle,[a] deg	idealized angle for D_{3h} geometry, deg
O2–O5–O10	O6–N2–O9	177.0(2)	180
O2–O5–O10	N1–N3–O12	173.5(2)	180
O6–N2–O9	N1–N3–O12	174.1(2)	180
O9–O10–O12	N2–O5–N1	138.2(2)	146.4
O2–O6–O12	O5–N2–N3	141.6(2)	146.4
O2–O6–N1	O10–O9–N3	140.1(2)	146.4
O2–O6–O12	O2–O6–N1	20.5(2)	26.4
O10–O9–O12	O10–O9–N3	22.5(2)	26.4
O5–N2–N1	O5–N2–N3	17.4(2)	26.4

[a] Estimated standard deviations of last reported digit in parentheses.

Table 8. Longitudinal (r_1) and Transverse (r_2) Relaxivities of the Gd(III) Complexes of BOPTA, DTPA, and DOTA[a,b]

complex	r_1, $mM^{-1}\ s^{-1}$	r_2, $mM^{-1}\ s^{-1}$
$Gd\text{-}BOPTA^{2-}$	4.39 (0.01)	5.56 (0.02)
$Gd\text{-}DTPA^{2-}$	3.77 (0.01)	4.73 (0.02)
$Gd\text{-}DOTA^{-}$ [c]	3.56	4.75

[a] At 39 °C, 20 MHz, and pH 7.4. [b] Estimated standard deviations in parentheses. [c] From ref 29.

the triangular face of the trigonal prism containing only oxygens as donor atoms (about 0.2 Å closer). The $Gd-O_{water}$ bond is almost perpendicular to the mean plane described by O2–O6–O9–O10. The distance between the mean plane and the coordinated water molecules is 1.765(5) Å. The $Gd-O_{water}$ bond length (2.463(5) Å) is very similar to $Gd-O_{water}$ distances found in similar complexes with a water molecule in the inner coordination sphere of the metal ion.[3,28–30] Both the $Gd-O_{carboxylate}$ bond distances, ranging from 2.340(5) to 2.416(4) Å, and the Gd–N bond lengths, ranging from 2.571(5) to 2.800(5) Å, agree well with the coordination bond lengths in Gd(III)–polyamino polycarboxylate complexes.[3,28–30] The arrangement of BOPTA in $Gd\text{-}BOPTA^{2-}$ is quite similar to that of DTPA in the $Gd\text{-}DTPA{\cdot}H_2O{\cdot}Na_2$ complex.[3] Covalent and coordinating interatomic distances, apart from those involving hydrogen atoms, differ maximally by 0.09 Å, and the root mean square difference for these distances is 0.0277 Å. $Gd\text{-}BOPTA^{2-}$ seems also very similar to the Gd complex of DTPA-bis(ethylamide)[30] and the Dy complex of DTPA-bis(methylamide).[31] In $Gd\text{-}BOPTA^{2-}$ the carboxylic oxygen atoms that are not involved in the metal ion coordination point away from the coordination cavity, as does the benzyloxymethyl side chain.

Finally, in the crystal lattice, the sodium counterions are hexacoordinated by oxygen atoms belonging to ligand carboxylate groups of four different molecules and to the independent water molecule (O13). Pairs of sodium ions are cross-linked by two bridging oxygen atoms on carboxylate groups contributed by different molecules. The Na···O contacts range from 2.298(6) to 3.020(6) Å. In addition, a weak interaction exists between oxygen O13 of the crystallization water molecule and oxygen O12 of the Gd-coordinated water molecule (3.140(7) Å).

Water Proton Relaxation. The efficacy of $Gd\text{-}BOPTA^{2-}$ as a contrast agent for MRI has been preliminarily evaluated by measuring its effect on water proton relaxation times. The longitudinal and transverse relaxivity values of $Gd\text{-}BOPTA^{2-}$ at 20 MHz, 39 °C, and pH 7.4 are reported in Table 8 along with the corresponding values for $Gd\text{-}DTPA^{2-}$ and $Gd\text{-}DOTA^{-}$ complexes. The observed net paramagnetic relaxivity ($r_{1,obs}$) represents the sume of two contributions due to the inner ($r_{1,is}$) and outer ($r_{1,os}$) sphere mechanisms:

$$r_{1,obs} = r_{1,is} + r_{1,os}$$

The explicit forms of $r_{1,is}$ and $r_{1,os}$ are given by the Solomon–Bloembergen–Morgan[32–34] and Freed[35] equations, respectively. The theory of paramagnetic relaxation has been exhaustively described and applied to small metal complexes in several papers.[2,36] Nonetheless, it is worth remembering the following. (i) Inner sphere relaxation arises from the water molecules directly coordinated to the metal ion, and in fast exchange with the bulk water. This contribution depends on the number of coordinated water molecules, q, their residence lifetime, τ_m, the distance, r, between the protons of the q water molecules and the metal ion, the electronic relaxation time, τ_s, of the metal ion and the reorientational correlation time, τ_r, of the whole complex. (ii) Outer sphere relaxation contribution arises from water molecules diffusing near the paramagnetic complex. It depends upon the distance of closest approach, d, between the paramagnetic center and water protons, upon the sum of their diffusion constant, D, and upon τ_s. Furthermore, the electronic relaxation time is dependent on the magnetic flux density and is characterized by the correlation time τ_v, which describes the fluctuation of the electron spin–lattice interaction, and by the zero-field value τ_{s0}.

For compounds of similar size and structure, such as the Gd(III) complexes of BOPTA, DTPA, and DOTA, it can be assumed that the outer sphere mechanism makes a similar contribution at high magnetic flux densities (>0.1 T). Therefore the small differences in relaxivity shown in Table 8 can be ascribed to differences in $r_{1,is}$. The relaxivity values of the three complexes are of the same order of magnitude, indicating that there are the same number of exchangeable water molecules in the inner coordination sphere of these complexes. One exchangeable water molecule was found in the Gd(III) complexes of both DTPA and DOTA.[2] Luminescence studies of solutions have revealed 1.2 ± 0.5 coordinated water molecules in $Eu\text{-}BOPTA^{2-}$.[37] It may thus be safely assumed that also $Gd\text{-}BOPTA^{2-}$ in solution has one exchangeable water molecule (q = 1), namely that which also occupies one coordination site in the polyhedron around the gadolinium ion in the solid state.

From the X-ray crystal structure data for the Gd(III) complexes of BOPTA, DTPA, and DOTA, very similar values for the $Gd-O_{water}$ distance were found. Consequently, the differences in the relaxivity values must reflect differences in τ_r, the rotational correlation time that almost exclusively determines the relaxivity at high magnetic flux densities and that is related to the size of the complexes. A more accurate and quantitative analysis was pursued by recording the NMRD profile of the complex, i.e., by studying the dependence of the water proton longitudinal relaxation rate over a wide range of magnetic flux densities and corresponding Larmor frequencies.

Figure 6 compares the experimental NMRD profile of $Gd\text{-}BOPTA^{2-}$ with that of $Gd\text{-}DTPA^{2-}$. The equations for both inner and outer sphere relaxation[32–35] were fitted to the experimental data by using r, τ_r, τ_{s0}, and τ_v as adjustable parameters and by taking into account one coordinated water molecule (q = 1). The following values were taken from Koenig and Brown:[2] d = 3.6 Å and $D = 2.6 \times 10^{-5}\ cm^2\ s^{-1}$. For small Gd(III) chelates (except for Gd(III) complexes of DTPA-bis(amides)[38]) the mean residence lifetime τ_m does not

(31) Ehnebom, L.; Pedersen, B. F. *Acta Chem. Scand.* **1992**, *46*, 126.
(32) Bloembergen, N. *J. Chem. Phys.* **1957**, *27*, 572.
(33) Solomon, I. *Phys. Rev.* **1955**, *99*, 559.
(34) Bloembergen, N.; Morgan, L. O. *J. Chem. Phys.* **1961**, *34*, 842.
(35) Freed, J. H. *J. Chem. Phys.* **1978**, *68*, 4034.
(36) Koenig, S. H.; Brown, R. D. *Magn. Reson. Med.* **1984**, *1*, 478.

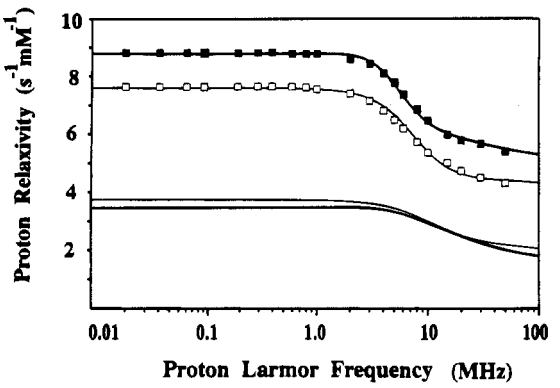

Figure 6. $1/T_1$ NMRD profiles of aqueous solutions of Gd-BOPTA (■ and thick lines) and Gd-DTPA (□ and thin lines) measured at 25 °C and pH 7.4. The lower curves represent the outer sphere contribution to proton relaxivity.

Table 9. NMR Parameters for Gd-DTPA^{2-} and Gd-BOPTA^{2-} Obtained from the Fitting of NMRD Profiles with the Inner Sphere Relaxation Theory[a]

	τ_{s0}, ps	τ_v, ps	τ_r, ps	r, Å
Gd-BOPTA^{2-} [b,c]	76 (2)	26 (1)	88 (2)	2.96 (0.02)
Gd-DTPA^{2-} [b,c]	82 (2)	19 (1)	73 (2)	3.07 (0.02)

[a] At 25 °C and pH 7. [b] According to Micskei *et al.*[39] τ_m = 200 ns was imposed in the fitting procedure. [c] Numbers in parentheses represent standard deviations in mean parameter estimates on 1000 simulated relaxivity data sets obtained by introducing repeatedly into the experimental data set random errors of 1% and estimating best parameters.

contribute significantly to the overall correlation time for the dipolar interaction and is often assumed to be on the order of the nanoseconds,[2] as found for the aquo ion. A τ_m value of 200 ns, as recently found by Micskei *et al.* in an ^{17}O NMR study for Gd-DTPA^{2-},[39] was used in our best fitting procedure. Of course this value represents an upper limit for τ_m since the actual value of this parameter cannot be evaluated by relaxometry. In fact the plot of ln R_{1p} vs $1/T_1$ in the range 2−60 °C at 20 MHz is a straight line, thus indicating that the fast exchange condition ($T_{1M} \gg \tau_m$) holds over the entire temperature range. The solid lines through the data points in Figure 6 were calculated from the best fit parameters reported in Table 9. The lower curves in Figure 6 represent the outer sphere contributions to the NMRD profiles. The relaxivity of Gd-BOPTA^{2-} is greater than that of Gd-DTPA^{2-} over the entire range of the investigated magnetic field. At high magnetic flux density the relaxivity ratio of the two complexes is equal to 1.27 (50 MHz). In this region, with the outer sphere contributions essentially identical, the relaxivity differences can be ascribed to the differential contribution of the inner sphere components. From the data plotted in Figure 6 the ratio between the inner sphere terms of Gd-BOPTA^{2-} and Gd-DTPA^{2-} reaches a value of 1.5. This value closely corresponds to the ratio between the τ_r/r^6 terms for the two complexes as expected for the dominance of τ_r in determining the relaxivities of small-sized Gd(III) complexes in the high magnetic flux density region. For Gd-BOPTA^{2-} both τ_r (~20% longer) and r (~4% shorter) contribute to enhance the relaxivity over that of Gd-DTPA^{2-}.

The longitudinal relaxivity ratio of the two complexes decreases from 1.27 at high magnetic flux density to 1.15 in the flat region at low magnetic flux density. This reflects the change in electronic relaxation time τ_s between the two complexes. In fact, a profile calculated by keeping constant the τ_s value found for the DTPA complex while the τ_r/r^6 term is altered does not agree accurately with the experimental data for Gd-BOPTA^{2-} in the low magnetic flux density region. From the fitting procedure it appears that the parameter chiefly responsible for this difference is τ_{s0} (i.e., the τ_{s0} value for Gd-BOPTA^{2-} is about 7% lower than that for Gd-DTPA^{2-}). Since τ_{s0} affects both the inner and outer sphere relaxivities, it follows that the outer sphere relaxation curve of Gd-BOPTA^{2-} is slightly lower than that of Gd-DTPA^{2-}.

However, the effects of such a difference for the inner sphere relaxivity are attenuated by the predominant role of τ_r in determining the relaxation behavior. A τ_{s0} decrease following a chemical modification of a chelate basic structure has already been observed for some gadolinium complexes of DOTA-like ligands; it has been attributed to a decreased symmetry of the first coordination sphere around the metal ion.[2,29]

In conclusion, despite the negative effect associated with a smaller τ_{s0} value, Gd-BOPTA^{2-} shows a greater water proton-relaxing ability than Gd-DTPA^{2-}, especially at magnetic flux densities relevant to MRI. It must be stressed that some of the calculated relaxation parameters of Table 9 likely are average values owing to the presence of different stereoisomers in solution (see below). According to Figure 6, at 20 MHz the one exchangeable water molecule in Gd-BOPTA^{2-} makes, through inner sphere relaxation mechanisms, a contribution of 3.40 mM^{-1} s^{-1} to the overall relaxivity, whereas outer sphere mechanisms contribute to the extent of 2.47 mM^{-1} s^{-1}.

Lanthanum-139 NMR Study. Among the lanthanides, only ^{139}La, with a receptivity which is 5.91% that of a proton, presents nuclear properties favorable for direct NMR spectroscopy. However, it has an $I = {}^7/_2$ spin and its electric quadrupole moment often leads to very broad resonances.

It has been demonstrated that ^{139}La chemical shifts are very sensitive to the number and type of ligand atoms in polyamino polycarboxylate complexes.[40] Hence, ^{139}La NMR can be used to investigate lanthanide coordination. The ^{139}La chemical shift measured for the La-BOPTA^{2-} complex of 246 ± 10 ppm (70 °C and pH 7.3) is very similar to that found for the La-DTPA^{2-} complex of 258 ± 4 ppm.[40] This strongly indicates that the two complexes have similar metal coordination structures in solution. However, the proposed empirical rules for the additive ^{139}La chemical shifts induced by oxygen and nitrogen ligands[40] do not agree well with the three nitrogen and five carboxylate oxygen atoms and one water oxygen atom in the first coordination sphere suggested by all other data. Nonetheless, this result supports the finding that the chemical modification that distinguishes BOPTA from DTPA does not alter the complexing properties of the ligand.

The ^{139}La line width is another parameter which provides useful qualitative information since it is related to both dynamic and structural features of the complex. For a quadrupolar nucleus the line width at half-height, $\Delta\nu_{1/2}$, is given by the eq 3, wherein $1/T_2$ is the transverse relaxation rate, I is the nuclear

$$\Delta\nu_{1/2} = \frac{1}{\pi T_2} = \frac{3\pi}{10}\frac{2I+3}{I^2(2I-1)}\chi^2\left(1+\frac{1}{3}\eta^2\right)\tau_r \qquad (3)$$

spin, and τ_r is the rotational correlation time.[41] $\eta = (q_{yy} - q_{xx})/$

(37) Anelli, P. L.; Balzani, V.; Prodi, L.; Uggeri, F. *Gazz. Chim. Ital.* **1991**, *121*, 359.
(38) (a) Aime, S.; Botta, M.; Fasano, M.; Paoletti, S.; Anelli, P. L.; Uggeri, F.; Virtuani, M. *Proceedings of the Society of Magnetic Resonance in Medicine*, 12th Annual Scientific Meeting, Aug 14−20, 1993, New York; Vol. 1, p 238. (b) Aime, S.; Botta, M.; Fasano, M.; Paoletti, S.; Anelli, P. L.; Uggeri, F.; Virtuani, M. *Inorg. Chem.* **1994**, *33*, 4707. (c) Gonzales, G.; Powell, D. H.; Tissières, V.; Merbach, A. E. *J. Phys. Chem.* **1994**, *98*, 53.
(39) Micskei, K.; Helm, L.; Brücher, E.; Merbach, A. E. *Inorg. Chem.* **1993**, *32*, 3844.

q_{zz} is the asymmetry parameter determined from the principal components, eq_{ii}, of the electric field gradient tensor, $e\mathbf{q}$ ($0 < \eta < 1$). $\chi = e^2qQ/h$ is the quadrupole coupling constant (in Hz), in which Q is the quadrupole moment of the distribution of unit charge (in m^2) corresponding to the quadrupole moment eQ (in Cm^2). Thus the observed line widths depend on the size of the complex through τ_r and on the symmetry of the ligand field through q_{zz} and η. The La-BOPTA^{2-} bandwidth is 9300 Hz, which is significantly broader than that of La-DTPA^{2-} (6300 Hz). If this difference were ascribed to the large value of τ_r for La-BOPTA^{2-} only, the τ_r value of La-BOPTA^{2-} would have to be 48% larger than that of La-DTPA^{2-}. This is at variance with the difference in τ_r of only 20% obtained from the fitting of the NMRD profile (Table 9).

The crystallographic results have shown that the coordination cage around the metal ion is essentially identical for Gd-BOPTA^{2-} and Gd-DTPA^{2-}. The same should hold for the corresponding La(III) complexes. Although line widths of quadrupolar nuclei vary strongly with changes in the symmetry of the environment,[41] it is questionable whether or not a variation in the ligand field symmetry (reflected in a significant increase in η and q_{zz}) of sufficient magnitude to explain the difference in ^{139}La line widths in the two complexes exists. Indeed, the line width difference may have to be explained in terms of the existence in solution of structural isomers with slightly different chemical shift values, isomers whose number, kind, and relative abundance may differ between the two complexes. The hypothetical existence of isomers was tested in a ^{13}C NMR study of diamagnetic La and Lu complexes.

Solution Structure and Dynamics of La- and Lu-BOPTA^{2-}. Some preliminary considerations may be of value in understanding the dynamics in solution of complexes involving BOPTA and lanthanide ions. Since lanthanide complexes of a certain ligand are generally almost isostructural, some basic assumptions can be made from what is known about Gd-BOPTA^{2-}. In the crystal, the benzyloxymethyl substituent was found on carbon C9 (Figure 4). Nothing precluded the substituent being found also on C11, C19, or C21 in solution or in another crystal form. Since the different structures are not interconvertible by simple rotation, this possibility alone shows the potential existence of four structural isomers. Taking into account the stereogenic carbon in the ligand, the number of possible stereoisomers for BOPTA complexes has to be doubled. Furthermore each of these eight stereoisomers can adopt two conformations depending on the helical (clockwise or anticlockwise) arrangement of the carboxylate groups about the gadolinium ion, as illustrated in Figure 7. In conclusion 16 possible stereoisomers for BOPTA complexes with lanthanide ions can theoretically exist. Obviously our crystallization procedure has selected a specific enantiomeric pair.

Lanthanide complexes of DTPA have previously been found to be in a state of dynamic interchange on the NMR time scale.[42-44] As Ln-BOPTA^{2-} complexes can be expected to show similar dynamics, one may envisage, in the fast-exchange limit, the detection of four couples of interconverting isomers (i.e. the eight possible conformers). Figure 7 schematically illustrates, for Gd-BOPTA^{2-}, such an equilibration process for one of these four couples.

To gain some insights into the solution structures and conformational dynamics of Ln-BOPTA^{2-} complexes, the

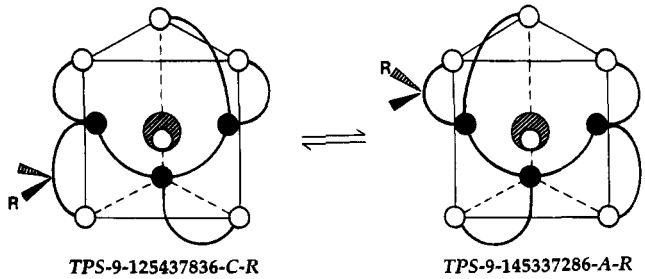

Figure 7. Schematic structures showing the equilibrium between two conformational isomers of Gd-BOPTA^{2-}: nitrogen atoms, solid circles; oxygen atoms, open circles; gadolinium ion, shaded circle. The structures are viewed along the pseudo-C_2 axis passing through the coordinated water molecule and the gadolinium ion. Below the structures are given the stereochemical descriptors according to the guidelines of *Chemical Abstracts*.[26]

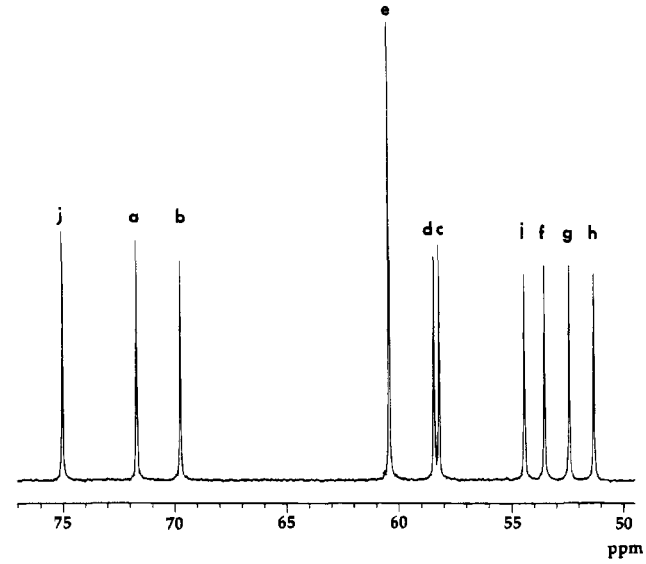

Figure 8. ^{13}C NMR spectrum (50–75 ppm range) of BOPTA in D_2O at pD_{app} 10.5 and 35 °C. Letters indicate peak assignments to carbon atoms as indicated in Figure 1.

BOPTA ligand and its diamagnetic La- and Lu-complexes were investigated by ^{13}C NMR spectroscopy. The NMR carbon spectrum of the ligand recorded at pD_{app} = 10.5 and 35 °C is reported in Figure 8: 10 aliphatic resonances were observed in the 50–80 ppm spectral region, which were unambiguously assigned on the basis of the ^{13}C–^{1}H coupling relationships from a 2D COSY experiment. Complexation with La(III) or Lu(III) causes remarkable temperature-dependent changes in the ^{13}C spectral pattern in terms of shift, splitting, and broadening of resonances. As expected, only the resonances of the *j* carbon were unaffected by temperature (Figure 9). The high-temperature spectra are consistent with the occurrence of either two static structures or two pairs of interconverting isomers. Upon a decrease in the temperature to 0 °C, several ^{13}C resonances markedly broaden. This indicates that a dynamic process is slowed at this temperture and supports the view that the observed spectral pattern is due to two or more couples of interconverting isomers. Unfortunately, the low solubility of Ln-BOPTA^{2-} complexes in water–methanol mixtures prevented recording the low-temperature-limiting spectra of the "frozen" structures. For the related Ln(III) complexes of the bis-(propylamide) of DTPA, Geraldes et al.[45] obtained enough evidence to ascertain the occurrence, in the high-temperature-limiting spectrum, of all the expected couples of interconverting

(40) Geraldes, C. F. G. C.; Sherry, A. D. *J. Magn. Reson.* **1986**, *66*, 274.
(41) Harris, R. K.; Mann, B. E. *NMR and the Periodic Table*; Academic Press: London/New York, 1979.
(42) Aime, S.; Botta, M. *Inorg. Chim. Acta* **1990**, *177*, 101.
(43) Jenkins, B. G.; Lauffer, R. B. *Inorg. Chem.* **1988**, *27*, 4730.
(44) Peters, J. A. *Inorg. Chem.* **1988**, *27*, 4686.
(45) Geraldes, C. F. G. C.; Urbano, A. M.; Alpoim, M. C.; Hoefnagel, M. A.; Peters, J. A. *J. Chem. Soc., Chem. Commun.* **1991**, 656.

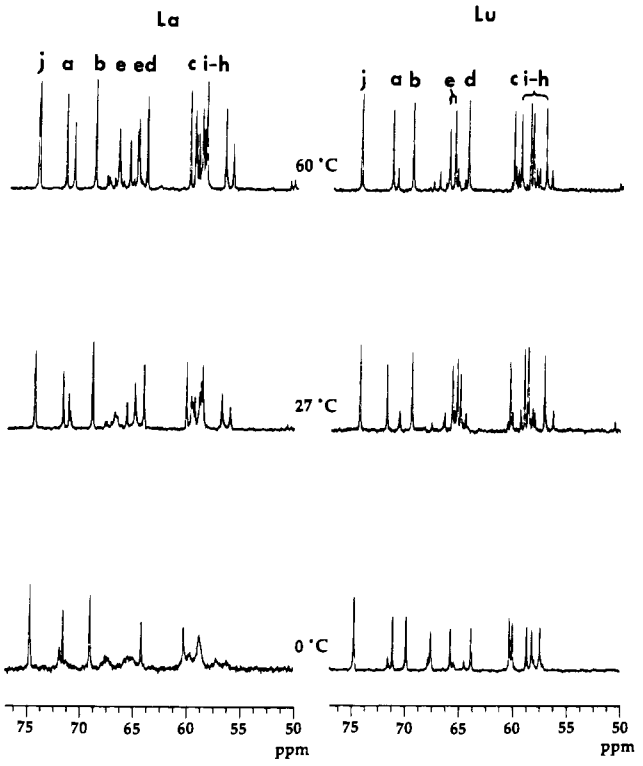

Figure 9. ^{13}C NMR spectra (50−75 ppm range) of La-BOPTA^{2-} and Lu-BOPTA^{2-} at various temperatures in D_2O (for labeling see Figure 1).

isomers. In the case of Ln-BOPTA^{2-} complexes, only two of the four expected couples were detected. Obviously a larger number of interconverting isomers could be hidden by superimposition of signals. More likely, the smaller number observed reflects the steric and electronic demands of the benzyloxymethyl substituent on the thermodynamic stabilization of some stereoisomeric pairs. Unfortunately the available NMR data do not allow any speculation on the structures of the isomers present in solution.

On a qualitative basis, at least, the observed temperature dependence of the ^{13}C resonances of these diamagnetic complexes of BOPTA shows that the bulky substituent in this chelator does not dramatically alter the nature or the rate of the dynamic process previously reported for complexes of the parent chelator, DTPA. Finally, it is worth noting that, in the case of the parent Ln-DTPA^{2-} complexes, the interconversion involves enantiomeric pairs whereas, in Ln-BOPTA^{2-} complexes, the same dynamic process averages out couples of conformers of opposite helicities which are not enantiomerically related.

Conclusions

Taken together, the data presented indicate that Gd-BOPTA^{2-} shares many properties with Gd-DTPA^{2-}. Apparently, substitution of one hydrogen atom with a benzyloxymethyl group on a terminal acetic acid residue does not significantly alter the ability of the compound to coordinate Gd(III). In particular, the similarity of the protonation and stability constants supports the expectation of similar stabilities in vivo. Should release of Gd(III) ions indeed be the cause of acute intravenous toxicity, as suggested by Cacheris *et al.*,[46] Gd-BOPTA^{2-} and Gd-DTPA^{2-} should have similar LD_{50} values. Indeed Gd-BOPTA^{2-} is slightly less toxic than Gd-DTPA^{2-}.[47]

The benzyloxymethyl group was found in the crystal to be in an extended conformation. If true in solution, this would favor the function of this moiety as a mediator for Gd-BOPTA^{2-} recognition by the bilirubin transporter.[48] This, in turn, facilitates its uptake into hepatocytes.[47]

Acknowledgment. We thank Drs. F. Bertani and A. Maiocchi for statistical help and Dr. M. Kirchin for the critical linguistic revision of the manuscript.

Supplementary Material Available: Tables S1−S3, listing thermal parameters, derived hydrogen positions, and angles and distances associated with the ligand anion (4 pages). Ordering information is given on any current masthead page.

IC940616N

(46) Cacheris, W. P.; Quay, S. C.; Rocklage, S. M. *Magn. Reson. Imag.* **1990**, *8*, 467.
(47) Cavagna, F.; Tirone, P.; Felder, E.; de Haën, C. Proceedings of the 2nd Special Topic Seminar: New Developments in Contrast Agent Research, Bordeaux, France, Sept 26−28, 1990. In *New Developments in Contrast Agent Research*; Rinck, P. A., Muller, R. N., Eds.; European Magnetic Resonance Forum: Blonay, Switzerland, 1991; pp 83−94.
(48) Lorusso, V.; Luzzani, F.; Tirone, P.; de Haën, C. *Book of Abstracts*; ECR '93, 8th European Congress of Radiology, Vienna, Austria, Sept 12−17, 1993; p 352.

Effects of Ortho-Substituents in the Synthesis and Stability of Cyclomanganated Benzylamine Derivatives. X-ray Crystal Structure of $Mn\{C_6H_2(OCH_3)_2$-4,6-CH_2NMe_2-2$\}(CO)_4$†

Michel Pfeffer* and Esteban P. Urriolabeitia

Laboratoire de Synthèses Métallo-Induites (URA 416 du CNRS), Université Louis Pasteur, 4 rue Blaise Pascal, F-67070 Strasbourg Cedex, France

Jean Fischer

Laboratoire de Cristallochimie (URA 424 du CNRS), Université Louis Pasteur, 4 rue Blaise Pascal, F-67070 Strasbourg Cedex, France

Received June 14, 1994⊗

The reaction of $PhCH_2Mn(CO)_5$ with several tertiary amines such as 8-methylquinoline, *N,N*-dimethyl-1-naphthylamine, or mono- and disubstituted *N,N*-dimethylbenzylamine derivatives, in refluxing *n*-hexane, affords the corresponding neutral C,N-cyclometalated Mn(I) compounds of stoichiometry Mn(C-N)$(CO)_4$, **1**−**8** (C-N = cyclometalated ligand), in good yields. These new compounds have been characterized by their IR and ^1H and $^{13}C\{^1H\}$ NMR spectra. The crystal structure of $Mn(C_6H_2(OCH_3)_2$-4,6-CH_2NMe_2-2$)(CO)_4$, **4** (monoclinic, $P2_1/n$; $a = 13.644$ (4) Å, $b = 9.153$ (3) Å, $c = 14.432$ (4) Å, $\beta = 115.57$ (2)°, $Z = 4$), shows the *N,N*-dimethylbenzylamine derivative to be coordinated as a chelating ligand and that the distance between the oxygen atom of the ortho OMe group and the carbon atom of one carbonyl group is shorter than the sum of their van der Waals radii. The orientation in the cyclometalation of benzylamine derivatives, when two possibilities exist, tends to avoid the steric interaction between the R groups ortho to the Mn−C bond and a CO unit. However, when this R group is OMe, the latter compound isomerizes so that the interaction between the O atom of the methoxy unit and the C atom of the CO can take place.

Introduction

The chemistry of organometallic compounds containing cyclometalated ligands is an area that is still interesting for many research groups throughout the world.[1] This is partly due to the fact that they have already been shown to be useful starting materials for organic synthesis.[2] Important progress was recently made in this direction, and it was shown that, besides palladium, several other metals have useful applications. Recently it was shown that cyclomanganated compounds[3] derived from aromatic ketones could lead to carbocyclization reactions in the presence of internal alkynes.[4] This has prompted several research projects toward related organomanganese compounds containing C,O- or C,P-coordinated ligands.[5] We recently showed that cyclometalated dimethylbenzylamine derivatives of palladium[2b,c] or ruthenium[6] lead to the synthesis of heterocycles when reacted with alkynes. As a continuation of this project, we have been interested in investigating whether cyclomanganated compounds derived from the same N-containing ligands might display similar behavior. Hence a prerequisite was to synthesize the required starting materials.

In spite of the extensive development in the synthesis of C,N-cyclometalated azobenzenes or other N-containing ligands with manganese,[7] little attention has been directed toward the synthesis of compounds containing C,N-coordinated *N,N*-dimethylbenzylamine ligands and, with the exception of Mn-

† This paper is dedicated to Prof. E. Lindner in honor of his 60th birthday.

⊗ Abstract published in *Advance ACS Abstracts,* January 1, 1995.

(1) Ryabov, A. D. *Chem. Rev.* **1990**, *90*, 403.

(2) (a) Ryabov, A. D. *Synthesis* **1985**, 233. (b) Pfeffer, M. *Recl. Trav. Chim. Pays-Bas* **1990**, *109*, 567. (c) Pfeffer, M. *Pure Appl. Chem.* **1992**, *64*, 335.

(3) Treichel, P. M. *Comprehensive Organometallic Chemistry*; Pergamon: Oxford, U.K., 1982; Vol. 4, pp 1−159.

(4) (a) Liebeskind, L. S.; Gasdaska, J. R.; McCallum, J. S.; Tremont, S. J. *J. Org. Chem.*. **1989**, *54*, 669. (b) Cambie, R. C.; Metzler, M. R.; Rutledge, P. S.; Woodgate, P. D. *J. Organomet. Chem.* **1990**, *381*, C26. (c) Cambie, R. C.; Metzler, M. R.; Rickard, C. E. F.; Rutledge, P. S.; Woodgate, P. D. *J. Organomet. Chem.* **1992**, *425*, 59. (d) Cambie, R. C.; Metzler, M. R.; Rickard, C. E. F.; Rutledge, P. S.; Woodgate, P. D. *J. Organomet. Chem.* **1992**, *426*, 213. (e) Cambie, R. C.; Metzler, M. R.; Rutledge, P. S.; Woodgate, P. D. *J. Organomet. Chem.* **1992**, *429*, 41. (f) Cambie, R. C.; Metzler, M. R.; Rutledge, P. S.; Woodgate, P. D. *J. Organomet. Chem.* **1992**, *429*, 59.

(5) (a) McKinney, R. J.; Firestein, G.; Kaesz, H. D. *Inorg. Chem.* **1975**, *14*, 2057. (b) Cooney, J. M.; Gommans, L. H. P.; Main, L.; Nicholson, B. K. *J. Organomet. Chem.* **1987**, *336*, 293. (c) Cooney, J. M.; Gommans, L. H. P.; Main, L.; Nicholson, B. K. *J. Organomet. Chem.* **1988**, *349*, 197. (d) Robinson, N. P.; Main, L.; Nicholson, B. K. *J. Organomet. Chem.* **1988**, *349*, 209. (e) DeShong, P.; Sidler, D. R.; Rybczynski, P. J.; Slough, G. A.; Rheingold, A. L. *J. Am. Chem. Soc.* **1988**, *110*, 2575. (f) Robinson, N. P.; Main, L.; Nicholson, B. K. *J. Organomet. Chem.* **1992**, *430*, 79.

(6) Abbenhuis, H. C. L.; Pfeffer, M.; Sutter, J. P.; De Cian, A.; Fischer, J.; Li Ji, H.; Nelson, J. H. *Organometallics* **1993**, *12*, 4464.

(7) (a) Bruce, M. I.; Iqbal, M. Z.; Stone, F. G. A. *J. Chem. Soc. A* **1970**, 3204. (b) Bruce, M. I.; Goodall, B. L.; Iqbal, M. Z.; Stone, F. G. A. *J. Chem. Soc., Chem. Commun.* **1971**, 1595. (c) Bennett, R. L.; Bruce, M. I.; Goodall, B. L.; Iqbal, M. Z.; Stone, F. G. A. *J. Chem. Soc., Dalton Trans.* **1972**, 1787. (d) Bruce, M. I.; Goodall, B. L.; Stone, F. G. A. *J. Organomet. Chem.* **1973**, *60*, 343. (e) Bruce, M. I.; Goodall, B. L.; Stone, F. G. A. *J. Chem. Soc., Chem. Commun.* **1973**, 558. (f) Bennett, R. L.; Bruce, M. I.; Goodall, B. L.; Stone, F. G. A. *Aust. J. Chem.* **1974**, *27*, 2131. (g) Bruce, M. I.; Goodall, B. L.; Sheppard, G. L.; Stone, F. G. A. *J. Chem. Soc., Dalton Trans.* **1975**, 591. (h) Bruce, M. I.; Goodall, B. L.; Matsuda, I. *Aust. J. Chem.* **1975**, *28*, 1259. (i) Bruce, M. I.; Bennett, R. L.; Matsuda, I. *Aust. J. Chem.* **1975**, *28*, 1265. (j) Bruce, M. I.; Goodall, B. L.; Stone, F. G. A. *J. Chem. Soc., Dalton Trans.* **1978**, 687. (k) Bruce, M. I.; Liddell, M. J.; Snow, M. R.; Tiekink, E. R. T. *Aust. J. Chem.* **1988**, *41*, 1407. (l) Little, R. G.; Doedens, R. J. *Inorg. Chem.* **1973**, *12*, 844.

0020-1669/95/1334-0643$09.00/0